Modelling the Lattice Parameter of Plutonium - Aluminium Solid Solution

Richard Darby

Abstract

Neural network modelling, a powerful method of non-linear pattern recognition, has been used to predict the lattice parameter of δ plutonium as a function of both aluminium concentration and temperature. The methods of producing such a model are explained and possible physical insights offered by the model are explored. Comparisons are drawn with an existing invar model and it is found that both agree on the general trends.

1. Introduction

Well known due to its attractive nuclear properties for energy production and nuclear explosives, the actinide plutonium is considered to be the most varied and interesting of all metals, with seven solid state phases known – more than any other element – and each phase exhibiting its own characteristics.

The presence of alloying elements increases this complexity further. Initial interest came as a result of the ability of alloying to stabilise high temperature phases of plutonium, in particular the δ phase at room temperature, allowing the fabrication of plutonium for use as fuel and weapons.

The variation of these plutonium alloys' lattice parameters with both temperature and solute addition is complicated, with coefficients of thermal expansion changing from positive to negative over a range of compositions and temperatures. These changes are not yet fully understood let alone easily predicted.

Any unexpected volume changes could compromise structural stability where plutonium alloys are contained by another material, leading to a serious health risk and a necessity to understand their behaviour.

Neural networks offer a non-linear modelling technique which can be used in problems where the physics are not fully understood, but in which oversimplification would be unacceptable.

Through the use of such neural networks, an attempt has been made to model plutonium's unique behaviour, enabling future predictions without the need for tests involving this dangerous nuclear material, as well as bypassing the need for structure determination by the complicated and time-consuming method of x-ray, neutron or electron diffraction.

2. Scientific Background

2.1 Pure Plutonium

Having only been discovered in 1941, plutonium research is still in relative infancy. As already mentioned, plutonium exhibits seven different solid phases. α, β, γ and ε all have very large, positive coefficients of thermal expansion (CTE) while the CTE of both the δ and δ′ phases are negative[1] (Figure 1). A further peculiarity of plutonium is the contraction upon melting as the liquid phase is denser than the ε, δ′ and δ phases (Table 1). Little is known of the complex seventh allotrope, ζ, which exists only at high

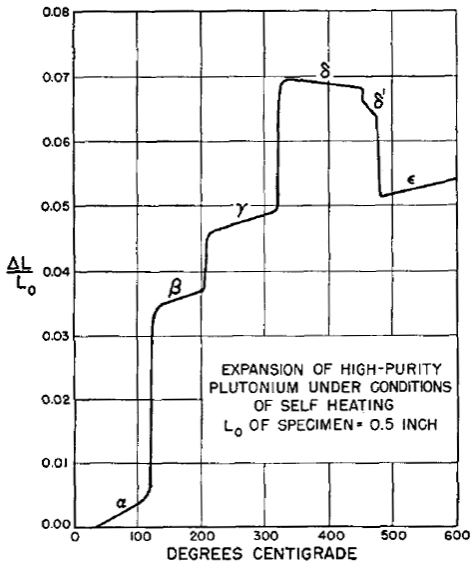

Figure 1: A dilatometer curve displaying the length change of a plutonium rod with temperature (image from Jette, 1955)

Phase	Crystal Structure	Density (g/cm^3)
α	Simple Monoclinic	19.86
β	Body-Centred Monoclinic	17.70
γ	Face-Centred Orthorhombic	17.14
δ	Face-Centred Cubic	15.92
δ′	Body-Centred Tetragonal	16.00
ε	Body-Centred Cubic	16.51
L	Liquid	16.65

Table 1: Some properties of the six ambient pressure phases.

temperatures and within a limited pressure range.

The electronic configuration of plutonium in the metallic state is $7s^2\ 6d^1\ 5f^5$ and it is suggested that these *f* electrons contribute to bonding in plutonium, causing some of its peculiar properties, namely low symmetry crystal structures, a high number of allotropic phases and a low melting point.

Initially the 'pointed' orbitals of the *f* electron wave functions were the cited cause[2], resulting in highly directional or covalent-like bonding favouring low symmetry crystal structures, this effect only being overcome at high temperatures, with the *f* character becoming smeared, permitting the cubic δ phase.

Within the last 15 years, due to increases in computing power, it has been possible to accurately calculate the total energy of the electronic ground state from first principals (without any experimental input). Wills and Eriksson applied this method to plutonium[3]. These calculations showed no localised increase in electron density between atoms, dismissing the possibility of covalent type bonding. Instead it was shown that in elements where a narrow *f* band straddles the Fermi energy level (as in the light actinides), the lifting of degeneracy associated with a less symmetrical crystal structure causes a splitting of the *f* band, an equal number being pushed both above and below the Fermi energy. This lowers the energy associated with the less than half filled *f* band of plutonium, stabilising 'distorted' crystal structures.

At present no calculations adequately predict the δ phase behaviour. The δ phase could be reproduced by Wills and Eriksson, but only by invoking a mixed state, where only one of the $5f^5$ electrons contributes to the bonding[3].

It is important to note that these first principal calculations only currently apply for zero temperature, and building in temperature dependence will be no simple task.

2.2 Plutonium Alloys

The combination of a large CTE and brittle crystal structure made the room temperature α phase undesirable for fabrication and use in a nuclear weapon (the

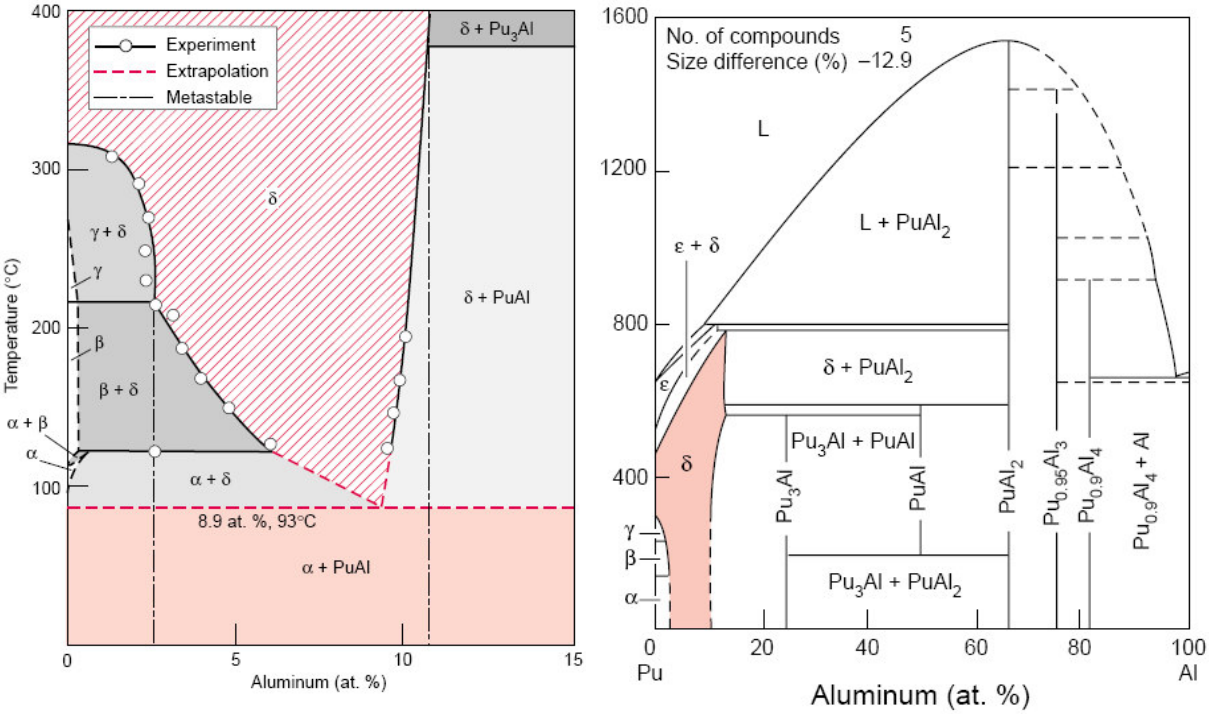

Figure 2: The phase diagram on the left (image from Hecker and Timofeeva, 2000) was determined by the Russians via acceleration of kinetics with preconditioning treatments. On the right is the phase diagram, previously believed to be correct in the West (image from Hecker, 2000), showing δ stabilisation to room temperature. Recently these two diagrams have been reconciled with the Russian version believed to be a true equilibrium diagram and the West's a good working diagram due to the slow kinetics.

production of which was the ultimate aim of early plutonium research). What was needed was the stabilisation of another, more malleable, phase.

It was found that a small addition of most trivalent elements (such as Ga, Al, Ce, Am, Sc, or In) retain the malleable δ phase to room temperature, with the trivalent element being incorporated in a solid solution of the plutonium fcc structure. This δ phase is actually metastable but due to exceedingly slow kinetics would take 10000 years to decompose at room temperature[4].

These slow kinetics have led to two plutonium–aluminium binary phase diagrams[4, 5] (Figure 2).

It is not understood what causes the trivalent elements to favour δ phase retention to ambient temperatures though the theoretical basis of a number phase diagram prediction models may provide insights[6].

Work on pure plutonium suggests that alloying elements could disturb the coherence of the 5*f* bands, much like increased temperature, leading to a reduction in the *f* electrons involved in bonding and a decreased drive for a distorted crystal structure[3].

Harrison's calculations show that stabilisation of the δ phase requires the cooperative effect of neighbouring solute atoms and will not occur when only considering just the sum effect of individual atoms[7].

2.3 Factors Affecting the Lattice Parameter of δ Plutonium

Commonly it is observed that materials expand upon heating. This is attributed to the asymmetric shape of the interatomic potential caused by strong nuclear repulsion forces, thus the average interatomic distance increases as atomic vibrations gain energy. Contrary to the predictions of this simple model, pure δ plutonium has a negative CTE, resulting in a reduction in lattice parameter with increasing temperature (Figure 1). It has been proposed that an invar model may be applied to explain this[8].

The "invar" property (that of invariable thermal expansion) was first seen in fcc Fe- 36Ni at.% whose CTE is essentially zero near room temperature. The invar model proposed the existence of two atomic states separated by an energy, Δ*E*, due to magnetic effects. As the temperature increased so would the population of the higher energy state, if this high energy state also possessed a smaller atomic volume then it is possible for its increasing occupancy to counter the normal

Figure 3: A schematic representation of the two atomic states in the two-state invar model. The higher energy state having a lower atomic volume (image from Lawson *et al*, 2003)

thermal expansion or even overcome it, resulting in a zero or negative thermal expansion (Figure 3).

For this model to apply to δ plutonium two analogous atomic states would have to exist, though no magnetic moments have been measured to date leaving the mechanism for producing these hypothetical states open to another possibility. Wills and Eriksson claim the invar model is consistent with their calculations[9].

Isothermal addition of aluminium shrinks the δ plutonium lattice[10]. The 12.9% size difference between atomic radii can only partially explain this. An additional contraction of the plutonium atoms is believed to be caused just by the presence of the aluminium atoms in the lattice.

In general it is thought that an increasing addition of aluminium results in an increasing number of 5*f* bonding electrons over the solitary electron calculated to be bonding in unalloyed δ plutonium[3]; leading to greater bonding and smaller atomic volumes. The exact mechanism remains inconclusive but one suggestion is that it is due to *f-p* bonding between Pu 5*f* and Al 3*p* bands[6].

Applying the invar model to lattice contraction by aluminium addition suggests that aluminium somehow stabilises the upper, smaller atomic state. Again the precise mechanism is unclear but the electronic interactions described in the previous paragraph are a possible candidate.

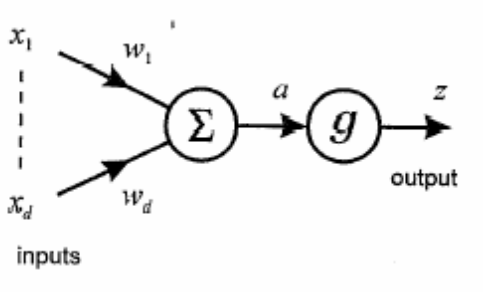

Figure 4: Representation of a single neuron in a neural network which forms a weighted sum of the inputs, x_i, and then transforms this sum using a non-linear activation function *g(a)* to give an output, *z* (image from Bishop, 1994)

3. Technique

Neural networks offer an alternative approach to materials modelling[11], instead of initially utilising an explicit set of assumed functional forms, the solution to a problem is obtained by fitting a very flexible non-linear function to a set of example data (hereafter referred to as training)[12]. This method bypasses the need to develop a first principles model of the underlying physical processes, as already achieved for unalloyed plutonium at 0 Kelvin[3]. The difficulties involved in extending this model to include alloying additions and temperature effects highlights the promise of using neural networks for modelling the lattice parameter of plutonium alloys.

The basic set up of a single neuron in a non-linear neural network regression is illustrated (Figure 4). The inputs, x_i, are the experimental variables (initially temperature and solute concentration for this model). Each variable is multiplied by a random weight, w_i, and then they are all summed together along with a random constant, w_0, known as the bias,

$$a = \sum_{i=1}^{d} w_i x_i + w_0 \qquad (1)$$

Optimising the constants to fit the example data after this step (training) would be sufficient if there was a linear relationship between the inputs and the output.

For non-linear relationships the randomly weighted input data is used in a non-linear 'activation function', commonly tanh,

$$z = \tanh(a) \qquad (2)$$

A weighted sum of the outputs of many neurons and a constant, $w_0^{(2)}$, is then trained to fit the example data to give the output value (lattice parameter in this model), y,

$$y = \sum_{j=1}^{n} w_j^{(2)} z_j + w_0^{(2)} \qquad (3)$$

where $w_j^{(2)}$ are the respective optimised weights and n is the number of neurons (also known as 'hidden units') used to fit the data.

The function usually chosen for the activation function (and the one used in this work) is the hyperbolic tangent due to its flexibility.

When training the model this study uses a method developed by MacKay[13]. Instead of simply identifying the best set of weights, a probability distribution of weights is calculated. When predictions are made a probability-weighted average of these weights is used. This quantifies the uncertainty of the fitting, allowing a quantitative measurement of the performance of the model. Using this method the performance of models is best evaluated using the log predictive error (LPE), which penalises wild predictions less if they are accompanied by a high uncertainty,

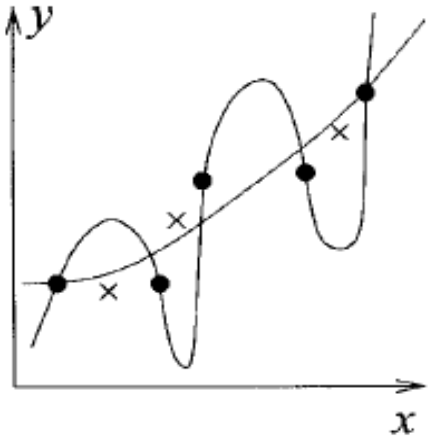

Figure 5: An overfitted model may fit the training data (●) perfectly but will have a larger test set (x) error than the optimum model (image from Sourmail *et al*, 2002)

$$\mathrm{LPE} = \sum_{m} \left[\frac{1}{2} \frac{(t^{(m)} - y^{(m)})^2}{\sigma_y^{(m)^2}} + \log\left(\sqrt{(2\pi}\sigma_y^{(m)})\right) \right] \qquad (4)$$

Where $t^{(m)}$ are the measured values, $y^{(m)}$ the corresponding predicted values and $\sigma^{(m)}$ are the error bars calculated using Bayesian statistics. A larger LPE implies a better model.

Once a set of weights has been determined for the example data, they can be used to make predictions on inputs for which outputs are not currently known.

As neural networks are extremely flexible, there is also the potential for overfitting[14] (Figure 5). A training dataset can be fit perfectly but the model will then generalise poorly beyond the input dataset. This problem is avoided by splitting the dataset randomly in two, a training set and a testing set. All models are trained on the training set and then used to make predictions on the unseen testing set, an overfitted curve will predict badly on the testing set and so will not be used in the final model. Also, complex models (high number of hidden units, large weights) are penalised by the existence of the objective function.

Due to the dependence of a model's final prediction on the number of hidden units and the initial random guesses for the weights, optimum predictions are often made by using the average prediction of more than one model. The performance of a cumulative number of 'sub-models' is tested against the testing set and the number that gives a minimal error forms a committee that is retrained on the full database and then used as the final model.

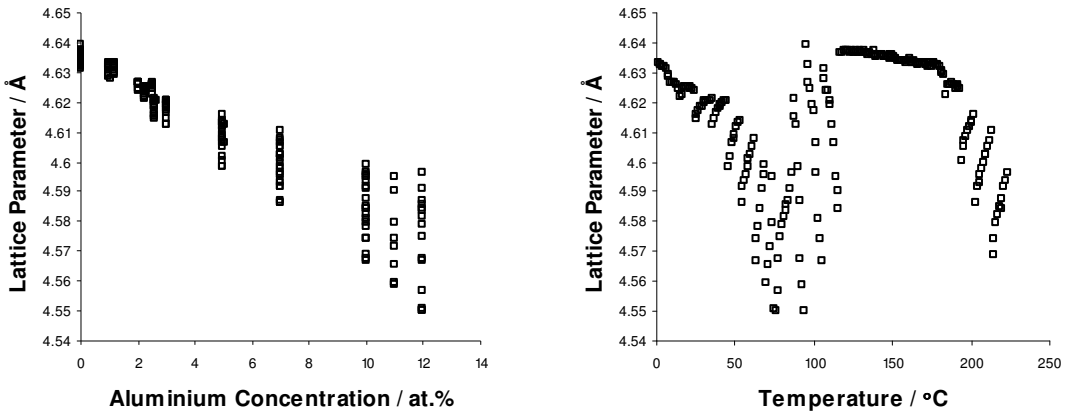

Figure 6: The distributions of the inputs, aluminium concentration and temperature, against the resultant δ plutonium lattice parameter.

4. Dataset

All 223 data points for Pu-Al and pure Pu used to train and test the models were acquired from literature[10, 15, 16] (Appendix 1). Most data points were digitised from published graphs using Engauge Digitizer[17]. Of the two sources that gave errors for the measured lattice parameter the greatest was ±0.0003 Å. Some rudimentary experiments with Engauge Digitizer found the error associated with reading the data was comparable with a value of ±0.0002 Å.

All concentrations are assumed to be absolute as only one reference described the Pu-Al specimen preparations where initial elemental weights were used to give the composition and verified by "negligible" weight loss after alloying[16].

The dataset variables are temperature (in °C) and aluminium content (in at. %) giving the output of lattice parameter (in Å). The range of these variables used for training the models (Table 2) and their distributions are given (Figure 6). Some data points lie outside the metastable δ phase field given by the phase diagram (Figure 2). This fact is acknowledged by the experimenters who assert the validity of the results due to no evidence of decomposition.

Variable	Min	Max	Mean	Standard Deviation
Al (at.%)	0.00	12.00	4.02	4.00
Temperature (°C)	6.64	572.46	300.42	135.73
Lattice Parameter (Å)	4.55	4.64	4.61	0.02

Table 2, the range of initial data points in the model's database

5. Computing Methodology

5.1 Early Models

Initially models were assessed by plotting the lattice parameter against temperature for a range of compositions for which experimental data existed in the dataset. An example of an early model's predictions is given (Figure 7). This appears to be a good approximation to the behaviour of δ plutonium's lattice parameter exhibiting the main trends, though there is a particularly poor fit with the 3 at.% Al data. This is possibly due to the high density of experimental data points in the high temperature region leading to improved fitting of this part of the curve while sacrificing the fit for lower temperatures. There appeared to be little variation in the quality of this fit when varying the amount of data retained for the testing phase of model training (between 10% and 50%).

Several steps were taken to refine the models produced. The fitting noise was reduced to more closely represent the experimental error. This resulted in a closer fit being attempted without trying to fit better than the error associated with the data. This obviously resulted in a better fit and lower uncertainties when matching the input data points (Figure 8) (the model's uncertainties are typically represented by error bars but they have been omitted from Figures 7 and 8 for improved clarity of predictions).

The model achieved this improved fit on every point in the training set by increasing its complexity. The effect of this increased complexity can be seen by comparing the high temperature extrapolations of both models (Figures 7 and 8). Whereas the first model has smooth and intuitively believable extrapolations, the extrapolations of the model with reduced fitting noise do not seem to follow the pattern set by the experimental data, varying wildly and with high uncertainty when there is no experimental data to constrain them. This inability to extrapolate makes the second model a bad model.

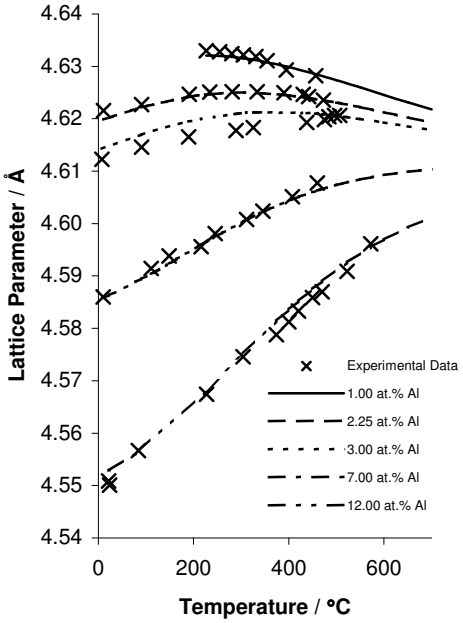

Figure 7: A plot comparing an early model's predictions with experimental data that was present in the model's dataset.

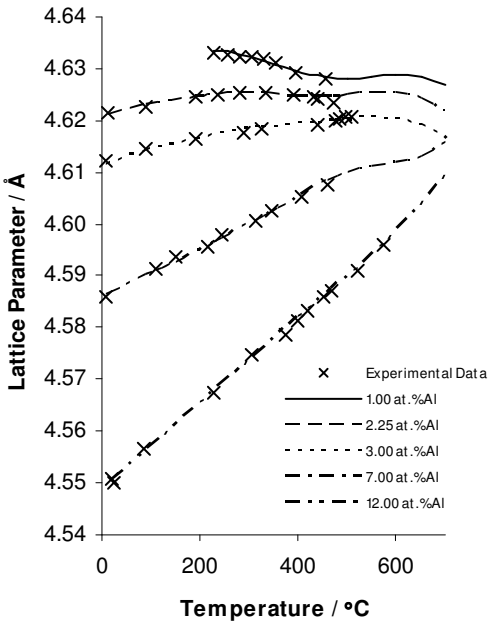

Figure 8: This model was prepared the same way as the first model (Figure 7) but the fitting was constrained in an attempt to more closely follow the data

5.2 Incorporating Perceived Influences

The suggestion that a cooperative effect of solute atoms contributed to the variation of lattice parameter[7] was included in the neural network model by using a quasichemical solution model representing the amount of clustering (preference for A-A bonds) or ordering (preference for A-B bonds) of the solute atoms, given by,

$$N_{AB}^{e} = \frac{zN[-1+[1+4x(1-x)(\exp\{2\omega/kT\}-1)]^{1/2}]}{2(\exp\{2\omega/kT\}-1)}$$

Where N_{AB}^{e} is the equilibrium number of AB bonds in a solution of A and B atoms, x is the concentration of A, and ω is a constant which is greater than 1.

Rather than just assuming a random solution this model allows calculation of the equilibrium number of unlike bonds due to enthalpy considerations. The input added to the model to represent this was proportional to N_{AB}^{e}, and so representative of the number of Pu-Al bonds.

This term is a function of both temperature and composition, both of which already exist as separate variables in the database. Including inputs that are functions of already existing variables is common practice where a known relationship is expected as it can help the network deduce this relationship.

Due to the form of this equation, a value of the constant ω had to be guessed. Several values were attempted, representative of different levels of clustering, but the models produced were similar for a range of ω values, a value of 2 was finally used.

Next the possibility of a two-state invar model was incorporated. Assuming the upper and lower states are separated by an energy difference ΔE, the population of the upper state, n_s, is given by

$$n_s = \frac{1}{1+(g_1/g_2)\exp(\Delta E/kT)} \qquad (5)$$

where g_1 and g_2 are the degeneracies of the upper and lower states respectively. g_1/g_2 is assumed to be one as we are lacking any evidence otherwise and the value of ΔE is $(1400/k_B)$ Joules as determined from a previous application of the invar model to the Pu-Ga system[18].

5.3 Rejected Influences

Assuming lattice misfit with the smaller aluminium atom was at least partly responsible, an average atom size input was introduced (the average was determined by the relative amounts of each atom and their atomic sizes in pure fcc Pu/Al). The network allocated this input virtually the same weight as that of aluminium concentration for every model it trained. This is a predictable result as the average atom size is proportional to the aluminium concentration and so inclusion of this variable allowed no extra insight.

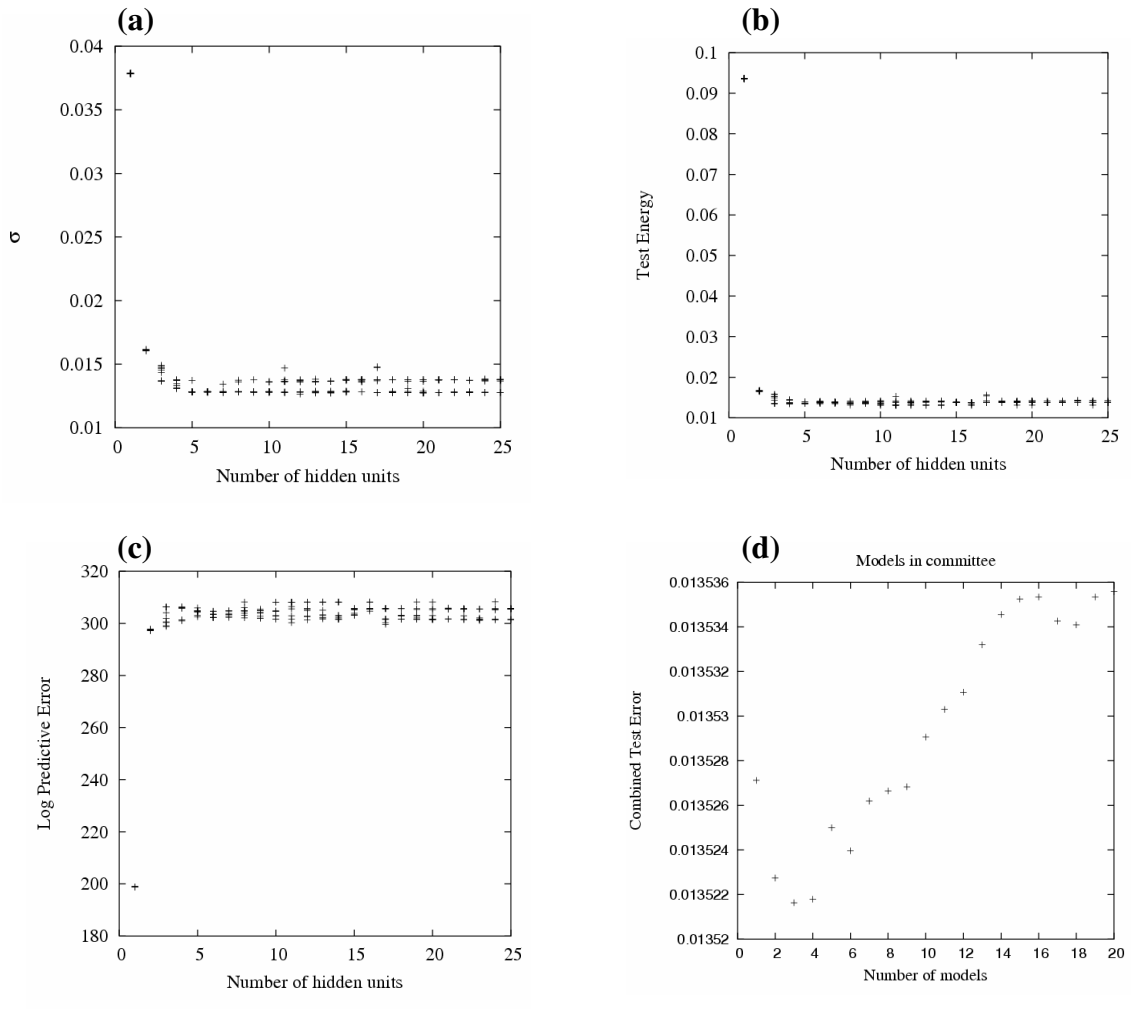

Figure 9: (a) The perceived level of noise of each sub-model plotted against the number of hidden units.
(b) Test error variance with number of hidden units.
(c) Log predictive error variance with number of hidden units.
(d) The cumulative test error for number of sub-models that will be included in the final committee.

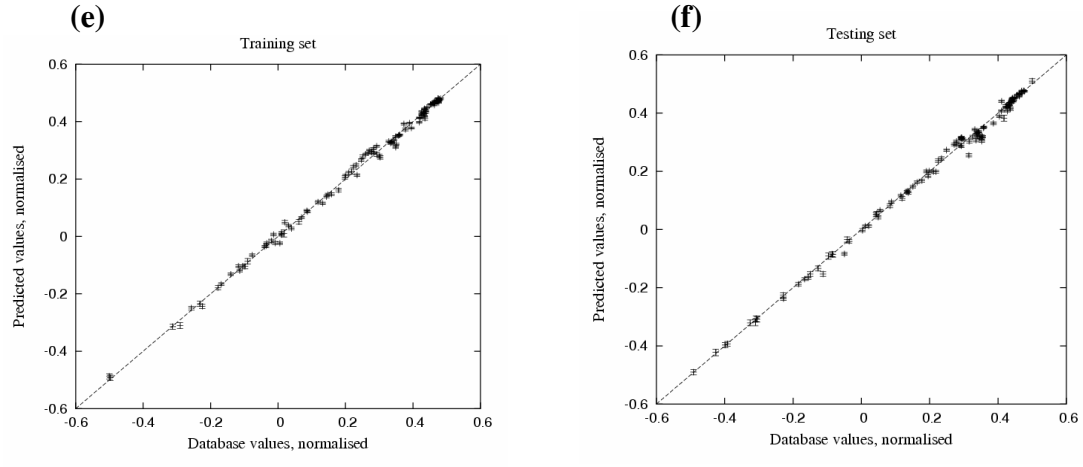

Figure 10: (e) The performance of the best single model in the committee on predicting the training set
(f) and the testing set.

6. Final Model Details

Both of the perceived influences in section *5.2* were included and 225 networks were trained with up to 25 hidden units and 9 different seeds. The constraint on the fit was the same as used for the first model reported (Figure 7), a relatively large ±30%. Predictably, the perceived level of noise decreases with an increasing number of hidden units as the model gains more flexibility to fit the data, this and other results of the training are illustrated (Figures 9 and 10). A committee of three models was chosen as it was a local minimum in combined test error and did not contain so many models that it risked averaging out some trends. The perceived significances of each of the inputs for the three models in the committee are shown (Figure 11). The significances represent the extent to which each input explains the variation in the output. The low significances accorded to temperature by two of the three models reflects the inclusion of temperature in the two functional inputs (quasichemical and invar).

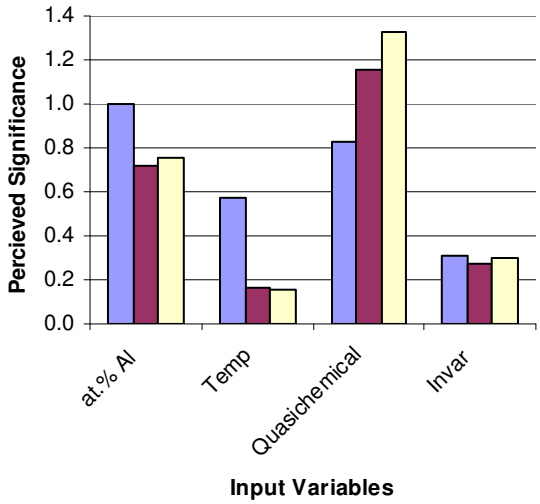

Figure 11: Perceived significances of the three networks constituting the final committee model.

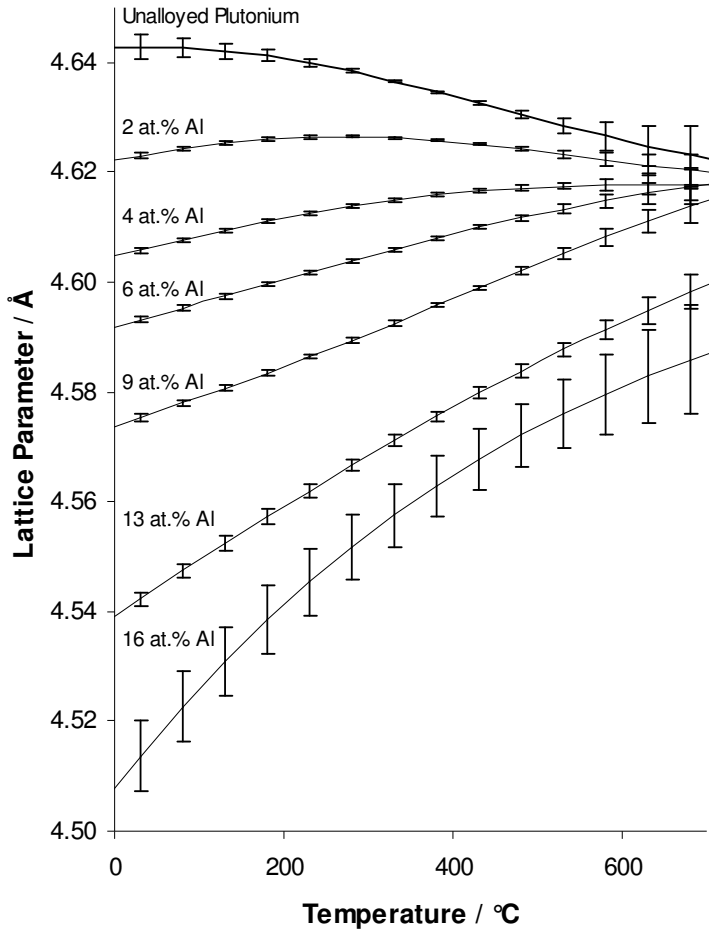

Figure 12: Predictions of the final model for δ plutonium's lattice parameter against temperature for a range of compositions. The error bars are indicative of the model's uncertainty in its prediction, with increasing uncertainty further beyond the limits of the initial inputs.

7. Evaluation of the Final Model

7.1 Model's Predictions

Incorporation of the perceived physical relationships described in section *5.2* allowed a better fit than the first reported model (Figure 7) without the need to constrain the fitting of the data, resulting in a simple, accurately fitting model that makes reasonable extrapolations.

When using this model for predictions, extrapolations will be made outside the metastable δ phase fields shown by the phase diagrams (Figure 2). Firstly for comparison with input data, as some points lie outside this region and secondly to see how the model behaves far away from the data it was trained on.

The final model's predictions for a selection of compositions are shown (Figure 12). When interpolating, the model predicts intuitive results along with low uncertainties, even for those compositions not explicitly included in the database. Greater uncertainties are associated with extrapolating both temperature and aluminium concentration, though both seem to follow the pattern set by the input data. An explanation of this pattern is attempted in section *7.2*.

A predicted lattice parameter-composition plot at varying temperatures is also given (Figure 13). The first obvious feature is the inversion in the order of the lines between 1.5 - 2 at.% Al due to the change in CTE from negative to positive with increasing aluminium concentration, as also illustrated in the experimental data (Appendix 1).

There is a general decrease in the susceptibility of the lattice parameter to aluminium addition with increasing temperature (decreasing slope gradient).

At low temperatures the line exhibits an upward curve at the lower solubility limit of aluminium and a downward curve at the upper limit, only the upward curve is reduced at high temperatures as the lattice parameter – composition variance tends to a straight line in the low aluminium region.

The general trends are in good agreement with the experimental data of Lee et al but are contradicted by the measurements of Ellinger, made beyond the upper solubility limit given in the phase diagram, which show an upward curve tending to a constant lattice parameter at room temperature[19] (Appendix 2). This data was not included in the dataset as it has not been officially published.

It was found that the fitting had vastly improved over early models due to the inclusion of the quasichemical term; this is reflected in the model's perceived significance of this input for all the networks used in the final committee. This suggests the possibility

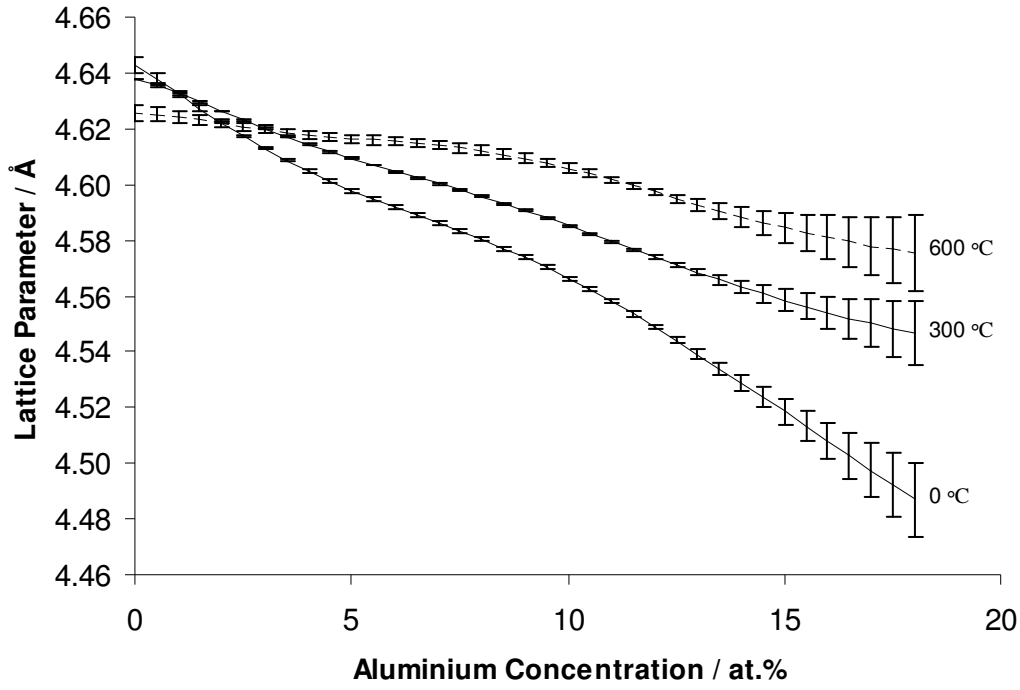

Figure 13: Predictions of the final model for δ plutonium's lattice parameter against composition for a range of temperatures. There is increasing uncertainty the further the composition extends above the upper limit in the initial database of 12 at.% Al .

of an important role of this variable in explaining the observed variance and thus an attempt will be made to explain the behaviour in terms of atomic ordering and the two-state invar model.

At higher temperatures the entropy of the system is increased, stabilising more random arrangements of atoms. If the effectiveness of the aluminium atoms to disturb the coherence of the plutonium *f* bands is related to a cooperative effect then a reduction in ordering should logically result in a reduction in aluminium's ability to reduce the lattice parameter, leading to the reduction in slope gradient with increasing temperature (Figure 13).

This same trend can be explained equally as well using the invar model where an increase in temperature results in a greater population of the high energy – low atomic volume state, Therefore the role of the aluminium atoms as a high energy state stabiliser becomes increasingly redundant, mirrored in their decreasing ability to shrink the plutonium lattice.

Assuming that the invar model is accurate, and that one aluminium atom affects all 12 of its neighbouring plutonium atoms an explanation for the upward curve at low aluminium additions and low temperatures can also be envisaged

The variation of N_{AB}^{e} with composition is rapid for dilute additions of solute, as each added atom only has unlike neighbours resulting in a high rate of lattice shrinking with aluminium additions. As the concentration increases further, the proportion of unstabilised plutonium atoms decreases, and aluminium atoms begin to have an increasing number of aluminium neighbours in the lattice. Both of these decreases the amount of shrinkage further aluminium additions can cause.

This explanation does not fit the increased shrinkage at high concentrations predicted by the neural model but it is consistent with the upward curve found by Ellinger[19].

It would be forthright to place too much onus on the quasichemical term for the appearance of the low aluminium, upward curve without further experiment. Its high perceived significance does not necessarily mean that atomic ordering definitely has a crucial role but just that the model has successfully used the shape of the function provided to fit the variation in the experimental data. Secondly the experimental data of Lee *et al*[10] used in this study appears to exhibit more of a gap between two straight line fits at 2.25 at.% Al rather than a gradual upward curve, which if true would make the quasichemical influenced explanation given here both invalid and unable to explain the true complexity of the situation alone, for which an explanation has already been attempted[10]. It should be noted that the existence of this 'kink' is not conclusive[19] and any proposed explanations are purely speculative.

It should also be noted that removal of the Lee *et al* data from the dataset used to create models (a loss of 116 data points and only leaving 49 Pu-Al data points in) actually leads to predictions of the shape observed by Ellinger. This large dependence of the model on one set of contentious experimental data is a problem that only the inclusion of further experimental data (none of which is available at present) will help resolve.

7.2 Comparison with Other Models

Only one other model has been found for the lattice parameter variance with both temperature and solute composition for a δ plutonium alloy[18]. Although it is for the Pu-Ga system comparisons can be drawn as aluminium and gallium are both trivalent group 3 elements.

The Pu-Ga fit was calculated using an invar model that balanced thermal expansion with the occupancy of two theoretical states of different atomic volumes (Figure 14). The simplified equation for the lattice parameter requires knowledge of several key parameters including the Debye temperature and Grüneisen constants.

A direct comparison of the models can be made using the unalloyed plutonium predictions (Figure 16). The general shapes of the curves are in agreement with the neural network model predicting a higher lattice parameter at 0 K and a lower one at 1200 K. There is an obvious discrepancy between the experimental values used to fit these models as the invar model fits the neutron diffraction measurements used in their study but not the x-ray measurements used in this study and vice versa. This could be partially to blame for the lack of agreement.

The shape of the curves shows a competition between normal thermal expansion, dominant at low temperatures, and increased occupancy of the upper, smaller atomic volume state, dominant at high temperatures. According to the invar model, the stabilisation of the upper atomic state of plutonium by aluminium (effective even at low temperatures) results in a smaller contribution of temperature to increasing the upper state occupancy. Therefore the higher the concentration of aluminium, the greater the

temperature range over which thermal expansion is dominant.

The general trends exhibited by increasing gallium addition match those discovered here for aluminium (Figure 15). This is a positive result for the neural network model if it is reasonably assumed that the low temperature Pu-Al data behaves in a similar manner to the experimentally determined data for Pu-Ga (Figure 14).

It should be noted that these extrapolations for Pu-Al (including unalloyed Pu) are presented as purely theoretical though δ plutonium retention has been observed down to -125 °C with the addition of 2 at.% aluminium[20].

8. Conclusions

Neural network modelling is a flexible method of data pattern recognition. Knowledge of the potential problems (particularly overfitting) allows quick and accurate fitting of data enabling the prediction of unknown outcomes.

A neural network model was produced for predicting the variance of δ plutonium lattice parameter with both temperature and aluminium composition. The model fitted the experimental data well while producing smooth extrapolations that compared favourably with an existing model without the need to experimentally determine certain parameters.

It was shown here that the use of suspected relationships can greatly improve the ability of the model to fit the data well. Care needs to be taken when interpreting this relationship as the significances given for each input does not describe the magnitude of the effect the input has on the final output but how it helps to describe the overall variance.

Though acknowledging this, possible physical explanations for the high significances of the quasichemical terms were proposed (Figure 11). The direct relevance of the quasichemical model could arise from the requirement of a cooperative effect of aluminium to stabilise the δ phase, or due to each aluminium atom stabilising all 12 of its nearest neighbours leading to lower amounts of stabilisation when additional aluminium atoms have nearest neighbours that are already stabilised.

The power of neural networks lies in their ability to spot patterns in a given data set but to see these overall trends it is sometimes necessary to sacrifice the degree of fitting on the initial data (Figures 7 and 8).

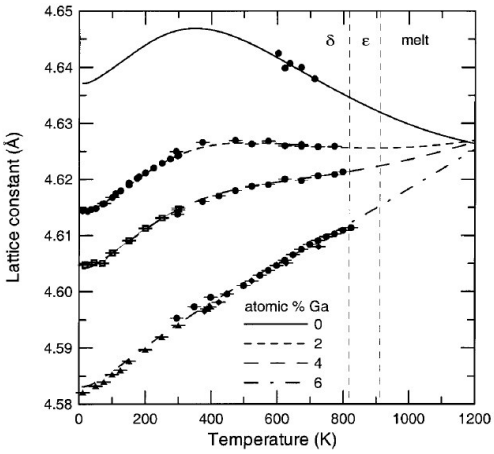

Figure 14: Variance of δ plutonium lattice parameter with temperature for a range of gallium concentrations predicted using the invar model, the circles represent experimental data (image from Lawson et al 1999).

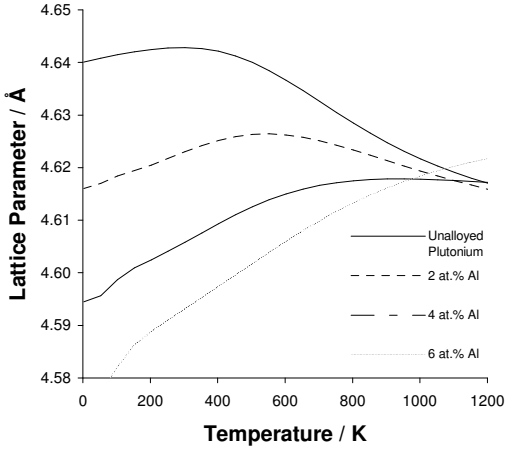

Figure 15: Variance of δ plutonium lattice parameter with temperature for a range of aluminium concentrations predicted using the neural network model of this study.

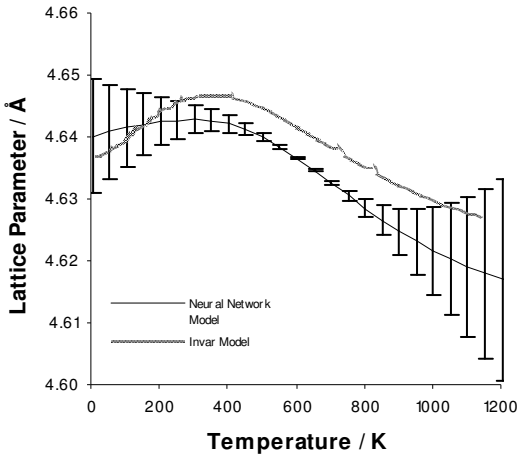

Figure 16: A direct comparison of the neural network and invar models' predictions for unalloyed plutonium.

When using a small database (as in this study) the flexibility of neural networks can result in the fitting of possible one-off experimental anomalies (Figure 13). This over complicates the model and can possibly lead to false extrapolations, highlighting the importance of considering the experimental inputs alongside the model's predictions.

The true power of neural networks becomes apparent when dealing with problems consisting of a large number of variables[14], here the ability to isolate certain variables and see how they affect the outputs can reveal new and interesting trends which were not previously realised. This power could not be exploited in the present study due to the small number of variables involved (fundamentally just temperature and composition) and the large range of existing experiments indicating how each variable varied when the other was held constant.

The variation of the lattice parameter across plutonium alloy systems presents an interesting challenge for neural networks. There exist several suspected influences that vary with alloying element, including the solute atom's size and electronic structure (occupied orbitals, orbital energies and Fermi energy level). A neural network approach may help isolate the most significant factors affecting lattice parameter and possibly even δ plutonium stability.

Acknowledgments

I would like to take this opportunity to thank Richard Kemp for his kind and patient supervision throughout the project and Prof. H. K. D. H. Bhadeshia for making it all possible.

References

1. E. R. Jette. *Some Physical Properties of Plutonium Metal*. The Journal of Chemical Physics **23** (2), 365-368 (1955).
2. R. D. Baker, S. S. Hecker & D. R. Harbur. *Plutonium—A Wartime Nightmare but a Metallurgist's Dream*. Los Alamos Science **4** (7), 142-151 (1983).
3. J. M. Wills & O. Eriksson. *Actinide Ground-State Properties—Theoretical Predictions*. Los Alamos Science **I** (26), 128-153 (2000).
4. S. S. Hecker & L. F. Timofeeva. *A Tale of Two Diagrams*. Los Alamos Science **I** (26), 244-251 (2000).
5. S. S. Hecker. *Plutonium and Its Alloys—From Atoms to Microstructure*. Los Alamos Science **II** (26), 290-335 (2000).
6. S. S. Hecker. *The magic of plutonium: 5f electrons and phase instability*. Metallurgical And Materials Transactions A-Physical Metallurgy And Materials Science **35A** (8), 2207-2222 (2004).
7. W. A. Harrison. *Theory of the electronic structure of the alloys of the actinides*. Physical Review B **6423** (23), art. no.-235112 (2001).
8. A. C. Lawson et al. *Applying the Two-State Invar Model to Delta-Phase Plutonium*. JOM **55** (9), 31-33 (2003).
9. O. Eriksson, J. D. Becker, A. V. Balatsky & J. M. Wills. *Novel electronic configuration in δPu*. Journal of Alloys and Compounds **287** (1), 1-5 (1999).
10. J. A. Lee, R. O. A. Hall, E. King & G. T. Meaden. *Some Properties of Plutonium and Plutonium-Rich Alloys* in Plutonium 1960: the proceedings of the Second International Conference on Plutonium Metallurgy, Grenoble, France, 19-22 April 1960 (ed. Grison, E.) 39-50 (Cleaver-Hume Press, London, 1961).
11. H. Bhadeshia. *Neural networks in materials science*. Isij International **39** (10), 966-979 (1999).
12. C. M. Bishop. *Neural Networks And Their Applications*. Review Of Scientific Instruments **65** (6), 1803-1832 (1994).
13. D. J. C. Mackay. *A Practical Bayesian Framework For Backpropagation Networks*. Neural Computation **4** (3), 448-472 (1992).
14. T. Sourmail, H. K. D. H. Bhadeshia & D. J. C. Mackay. *Neural network model of creep strength of austenitic stainless steels*. Materials Science and Technology **18** 655 (2002).
15. F. H. Ellinger. *Crystal Structure of Delta-Prime Plutonium And the Thermal Expansion Characteristics Of Delta, Delta-Prime, and Epsilon Plutonium*. Journal Of Metals **8** 1256-1259 (1956).
16. R. O. Elliott, K. A. G. Jr & C. P. Kempter. *Thermal Expansion of Some Delta Plutonium Solid Solution Alloys* in Plutonium 1960: the proceedings of the Second International Conference on Plutonium Metallurgy, Grenoble, France, 19-22 April 1960 (ed. Grison, E.) 142-155 (Cleaver-Hume Press, London, 1961).
17. *Engauge Digitizer*, http://digitizer.sourceforge.net/
18. A. C. Lawson, J. A. Roberts & B. Martinez. *Invar effect in Pu-Ga alloys*. Philosophical Magazine B **82** (18), 1837-1845 (2002).
19. F. W. Schonfeld. *Report* in Plutonium 1960: the proceedings of the Second International Conference on Plutonium Metallurgy, Grenoble, France, 19-22 April 1960 (ed. Grison, E.) 91-95 (Cleaver-Hume Press, London, 1961).
20. S. S. Hecker, E. G. Zukas, J. R. Morgan & R. A. Pereyra. *Temperature-Induced Transformation in a Pu--2.0 At.-% Al Alloy* in Solid to Solid Phase Transformations 1339-1343 (1982).

Appendix 1: Data Used in the Model's Database

Unalloyed δ plutonium from Ellinger (1956)

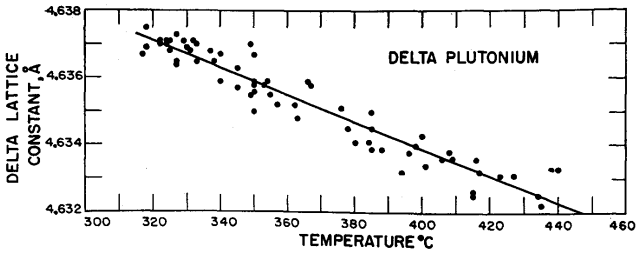

δ plutonium-aluminium alloys from Lee *et al* (1961)

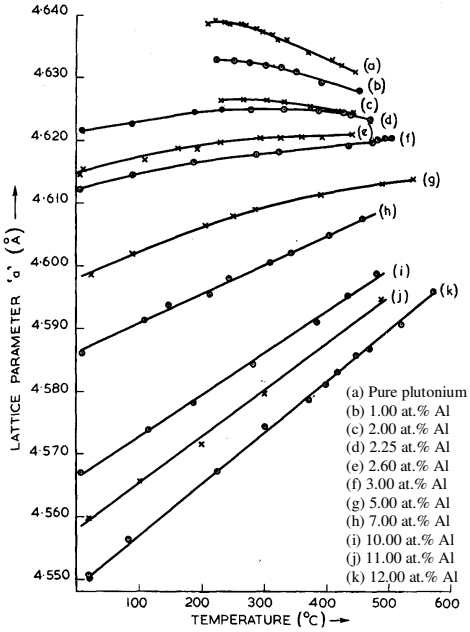

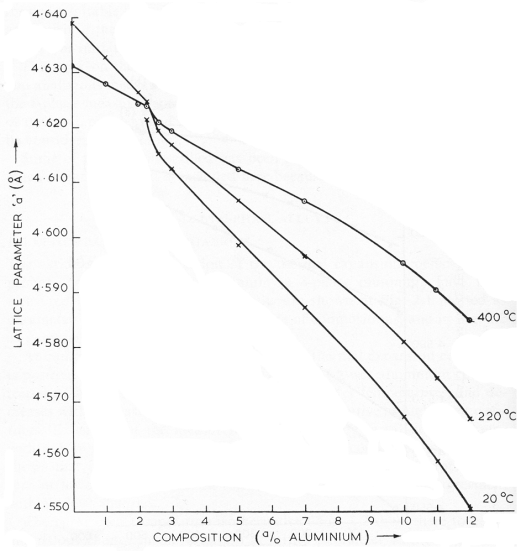

δ plutonium-aluminium alloys from Elliott *et al* (1961)

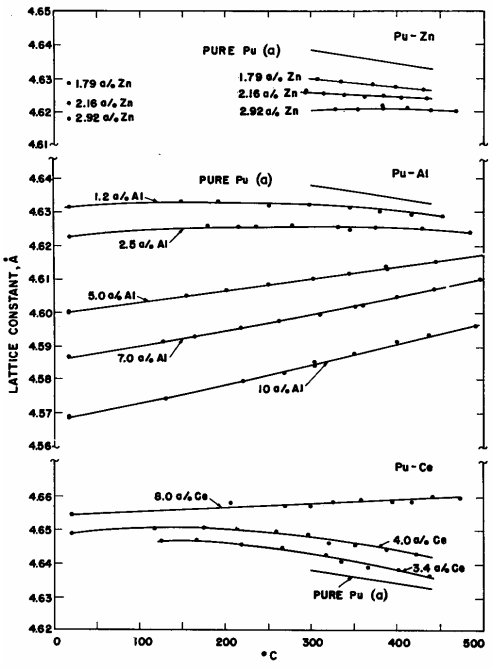

Appendix 2: Additional Data Not Used in the Model's Database

δ plutonium-aluminium alloys at 24 °C by Ellinger, reported by Schonfeld (1961)